Weather and Climate Extremes 37 (2022) 100474

Contents lists available at ScienceDirect

Weather and Climate Extremes

journal homepage: www.elsevier.com/locate/wace

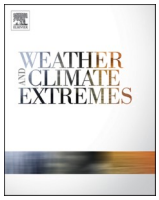

Convective environments leading to microburst, macroburst and downburst events across the United States

Djordje Romanic [a,*], Mateusz Taszarek [b,c,d], Harold Brooks [c,e]

[a] Department of Atmospheric and Oceanic Sciences, McGill University, Montreal, Quebec, Canada
[b] Cooperative Institute for Severe and High-Impact Weather Research and Operations, University of Oklahoma, Norman, OK, United States
[c] National Severe Storms Laboratory, Norman, OK, United States
[d] Department of Meteorology and Climatology, Adam Mickiewicz University, Poznań, Poland
[e] School of Meteorology, University of Oklahoma, Norman, OK, United States

A B S T R A C T

Downbursts are strong downdrafts of negatively buoyant air associated with convective storms and are capable of producing severe near-surface winds. Microbursts and macrobursts are subcategories of downbursts with the horizontal extent of damaging winds smaller or larger than 4 km, respectively. From January 2000 to June 2020, the Severe Weather Event Reports provided by the National Centers for Environmental Information (hereafter: Storm Events Database) contained 927 downburst, 914 microburst, and only 27 macroburst entries. We found a spatial variability of reported downbursts that is unlikely to be a result of natural processes, but rather artificially caused by the population density. An example of this bias is the abrupt decline in the number of reported events between southern and northern Arizona. Combining the Storm Events Database, ERA5 reanalysis and lightning data from the National Lightning Detection Network, we showed that cold pool strength, low-level lapse rates, WINDEX, lifted condensation level, DCAPE, WMAXSHEAR, derecho composite parameter, 2-m temperature, delta theta-e and mean low-level relative humidity demonstrate some value in downburst prediction. By combining the best predictor (cold pool strength) with the least correlated WMAXSHEAR, we created a downburst environment index (DEI) and used it to model climatological frequency of favorable downburst environments. Our analysis has shown that favorable downburst environments conditioned on lightning are the most frequent during summer over Southwest and Southeast with the most extreme environments across Great Plains. The vertical profiles of theta-e for the downburst events from reanalysis are further compared against nonsevere thunderstorms and rawinsonde data from four downburst field measurement campaigns. The results show that changes in theta-e over the lowest 200 hPa are the most important for downburst formation.

1. Introduction

The importance of reliable forecasts and climatology of severe thunderstorm winds spans across the disciplines of atmospheric sciences, energy and transportation, insurance, and wind engineering, to name a few. Despite this high demand, reports on severe convective winds are still incomplete and can be prone to errors and inaccuracies (Doswell et al., 2005; Trapp et al., 2006; Edwards et al., 2018). The spatiotemporal biases and uncertainties discussed in the literature are related to technological advancements over time, the spatial density of observations, subjective observational biases, variations in population density, damage reporting biases, as well as a combination of these factors (Kelly et al., 1985; Brooks et al., 2003; Romanic et al., 2016; Edwards et al., 2018; Taszarek et al., 2020a). As discussed in Kelly et al. (1985), non-trained people tend to report only the most spectacular events associated with thunderstorms and omit other phenomena. For example, if a thunderstorm spawned a tornado, then there is a tendency to only report that tornado and neglect other severe weather elements including severe nontornadic winds such as downbursts. Moreover, the damage inflicted by downbursts in these cases can often be assigned to tornadoes.

Severe nontornadic winds are considerably more frequent than tornadoes, both globally and regionally (Geerts 2001; Gensini et al., 2020; Taszarek et al., 2020b; Brown and Dowdy 2021; Pacey et al., 2021). In the United States (U.S.), severe winds are classified as those with the near-surface gusts exceeding 25.7 m s^{-1} (50 kt) whereas those that surpass 33.3 m s^{-1} (65 kt) are called significant severe winds (Brooks et al., 2003; Sherburn et al., 2016; Edwards et al., 2018). Nontornadic thunderstorm winds, which are often referred to as downdraft-associated winds, can be classified into straight-line winds caused by the high-pressure dome that forms in the precipitation zone and smaller-scale downbursts (Fujita 1981; Wakimoto 1985). Downbursts are further subdivided into microbursts and macrobursts depending on whether or not the horizontal extent of surface damaging

* Corresponding author. Room 849, Burnside Hall 805, Sherbrooke Street West, Montreal, Quebec, H3A 0B9, Canada.
E-mail address: djordje.romanic@mcgill.ca (D. Romanic).

https://doi.org/10.1016/j.wace.2022.100474
Received 26 August 2021; Received in revised form 15 June 2022; Accepted 17 June 2022
Available online 20 June 2022

winds is below or above 4 km, respectively (Fujita 1985). The smaller the spatiotemporal extent of the wind event, the more challenging the reliable reporting of that event can be. In addition, while only specific convective modes are supportive for producing tornadoes, nearly any thunderstorm is capable of generating strong downdraft-induced surface winds (Changnon 2001).

Therefore, creating a catalog of downbursts is, in principle, more challenging than tornadoes as less information on explicit reporting of these events is available. Namely, even if a tornado did not cause any significant damage, its presence is often clearly visible in the distance. The same does not apply for microbursts that often generate severe wind gusts in areas with low population density or in the regions where the potential for damage is often small (e.g., Great Plains). Changnon (2001) analyzed 892 property losses in the period 1949–1998 and not ed that while some thunderstorms in the U.S. caused the major damage by producing large hail, tornadoes, intense precipitation, and lightning, nearly all events were also accompanied with severe near-surface winds. Lombardo and Zickar (2019) showed that over 80% of annual maximum wind speeds over the central and southeast U.S. are caused by convective storms. They also found that in many regions where thunderstorm winds were not the most frequent type of extreme winds, they were still associated with the strongest gusts. As also noted by Taszarek et al. (2020b), among all thunderstorm-related hazards, severe convective winds have the shortest return periods conditioned on lightning occurrence over both the U.S. and Europe. Therefore, given that severe winds are likely the most common high-impact weather produced by convective storms, it is natural to expect that a large number of these wind events correspond to downbursts.

Downbursts are usually defined as negatively buoyant downdrafts that emerge from a thunderstorm cloud and impinge on the ground (Fujita 1985). The main contributing factors for downdraft development are evaporation (typically below ~1 km), melting (above ~1 km), and to a smaller extent also sublimation of hydrometeors (Knupp 1989). Other factors such as the precipitation loading, drag due to falling hydrometeors and pressure perturbations also play important roles (Wolfson et al., 1995; Richter et al., 2014; Childs et al., 2021). Access to considerable amounts of moisture also leads to strong downdrafts as it provides large latent heat released into the cloud and intensifies upward mass fluxes (James and Markowski 2010). To date, only four large field campaigns were designed specifically for downburst measurements in the U.S.. These are the Northern Illinois Meteorological Research on Downbursts (NIMROD; Fujita 1985) in the summer of 1978, the Joint Airport Weather Studies (JAWS; McCarthy et al., 1982) in the summer of 1982, the Federal Aviation Administration/Lincoln Lab Operational Weather Studies (FLOWS; Wolfson et al., 1987) in the summers of 1985 and 1986, and the Microbursts and Severe Thunderstorm project (MIST; Atkins and Wakimoto 1991) in the summer of 1986. A review of these early contributions to today's understanding of thunderstorm winds is provided in Burlando and Romanic (2020).

Multiple-Doppler radar and anemometer measurements from these field experiments provided the first observational data that triggered the early research on downburst dynamics (Wilson et al., 1984; Hjelmfelt 1988). Kelly et al. (1985) considered over 75,000 severe wind reports in the period 1955–1983 and created one of the first spatial maps of severe thunderstorm winds for the U.S.. After removing the wind reports from tropical cyclones and those not associated with deep moist convection (e.g., orographic winds), they reported that the central and northeast U.S. are the regions most prone to severe nontornadic winds (each with more than 14 thunderstorm wind occurrences per 26,000 km^2 per year). They also found that thunderstorm winds are most often in the late afternoon from May through summer. The JAWS program reported 168 microbursts over the 86 days of the field program near Denver, Colorado, and the diurnal variability of these events was similar to that found in Kelly et al. (1985). Over 80% of detected events were dry microbursts that were accompanied with little to no precipitation at the surface. The limited spatiotemporal extent of these and similar field campaigns prevents their straightforward generalization to other regions in the U.S..

Smith et al. (2013) developed a severe thunderstorm wind gust climatology for the period 2003–2009 for the contiguous U.S.. By separating wind gusts into those caused by supercells, quasi-linear convective systems and disorganized convective storms, the authors showed that there are several spatial patterns associated with different convective modes. For example, the supercell gusts were the most common east of the Rockies and in the plains. Kuchera and Parker (2006) compared over 500 model analyses to more than 7000 reports of severe convective winds for 2003 and concluded that the low-tropospheric winds were the most effective proxy for distinguishing between the environments that produced severe winds from those that did not. The diagnostic power of convective available potential energy (CAPE) and downdraft CAPE (DCAPE; Gilmore and Wicker 1998) was not as reliable as low-tropospheric winds. Their study also concluded that this subject deserves more research. By combining DCAPE and downdraft CIN (DCIN), Market et al. (2019) showed that the significant portion of severe near-surface winds was associated with small values of DCIN that enable the downdrafts to reach the surface. Taszarek et al. (2020b) investigated climatological characteristics of environments prone to severe thunderstorm hazards over Europe and the U.S.. They found that severe wind events over both continents were characterized by bimodal environments with cold season events occurring typically in high shear and low CAPE (HSLC) conditions, while summertime events were dominated by low shear and high CAPE (LSHC). Similar results concerning HSLC and LSHC severe convective wind environments were also found by Púčik et al. (2015), Sherburn et al. (2016), Gatzen et al. (2020) and Pacey et al. (2021). In another study, Romanic et al. (2020) analyzed the transient features of 41 thunderstorm wind records from around the world and found that the power spectral density of the U.S. events differs from the European records. In Australia, Brown and Dowdy (2021) used station reports and reanalysis data to show that methods based on environmental measures provide a better indication of the observed severe convective winds than the simulated model wind gusts from the reanalysis. They noted that severe convective winds were supported by steep mid-level tropospheric lapse rates, moderate convective instability, low relative humidity at near-surface and strong environmental wind speeds. Their results corroborate well with Kuchera and Parker (2006). However, none of the above studies distinguished between different types of thunderstorm winds, or focused on downbursts.

The severe weather event reports (hereafter referred to as Storm Events Database), provided by the National Centers for Environmental Information (NCEI), are a catalog of severe thunderstorm weather across the U.S. (Schaefer and Edwards 1999). While the reports are not flawless (Galway 1989; Edwards et al., 2018), they provide the most comprehensive high-impact and up to date severe storm database in existence. Each entry in a report contains a qualitative description that indicates the type of severe wind event or damage caused by the wind. While some wind events in the reports are explicitly classified as microbursts or macrobursts, others are categorized only as downbursts. This information on the specific type of a downburst is provided as a qualitative description of the given wind event. The two subcategories—microburst and macroburst—are assigned based on subjective interpretation of the people that reported the events. This type of subjective evaluation of a wind event is prone to errors because one cannot reliably measure outflow size by visually observing the event. Conversely, a large number of actual downburst events may be omitted by the lack of appropriate description of the event. Therefore, the goal of this paper is to improve our understanding of the convective environments prone to the development of downbursts across the U.S. and provide climatological estimates of proxies favoring their occurrence. We also evaluate differences in reports classified as microbursts and macrobursts. These objectives are accomplished by combining the Storm Events Database severe wind reports, ECMWF ERA5 reanalysis and National Lightning Detection

Table 1
Examples of microburst, macroburst and downburst entries in the Storm Events Database.

Date (local time)	State	Longitude, latitude	Episode narrative
1 August 2000 (17:25)	Wisconsin	−88.70°W, 43.30°N	An isolated severe thunderstorm pulsed up over central Dodge County and moved east at 10 mph. Downburst winds toppled several large trees.
11 August 2002 (16:05)	Wisconsin	−89.78°W, 43.15°N	The fringe effects of this powerful macroburst resulted in some tree damage north to the Cross Plains to Middleton area.
30 June 2016 (12:45)	Kansas	−95°W, 38.8°N	A 40 by 80 foot barn was destroyed by a microburst near Edgerton. Nearby power poles were also heavily damaged and 8–10 inch tree limbs were also torn off of trees.
30 May 2020 (16:55)	Utah	−113.2081°W, 40.0461°N	Afternoon thunderstorms developed across northern Utah and produced strong downburst winds.

Network (NLDN) lightning data.

2. Data and methodology

This study uses Storm Events Database severe wind reports from January 2000 to June 2020 (https://www.ncdc.noaa.gov/stormevents/ftp.jsp). These reports are obtained as a comma-separated (*.csv) files that contain all available observed storm events over that period (20 years and 6 months). Each file contains over 50 columns that provide various information, such as the beginning and end dates and times, unique event ID, location, deaths and injuries associated with the event, property damage, and so on, including a column named "*Episode Narrative*." This entry qualitatively describes the event beyond being just a thunderstorm wind, winter storm or similar, and in selected cases specifies if the reported wind event was considered as microburst, macroburst or simply a downburst without inferring its size. A few examples of these entries are provided in Table 1. In this study, we identified a total of 1868 events that were classified as either microbursts, macrobursts or downbursts, and combined them with proximal profiles from ERA5 reanalysis data (closest grid and closest timestep) to examine accompanying environments.

In addition to the trained meteorologists at the National Weather Services (NWS) and damage survey experts reporting and documenting the storm events, the information about storms and severe weather in the Storm Events Database may also be provided by or gathered from

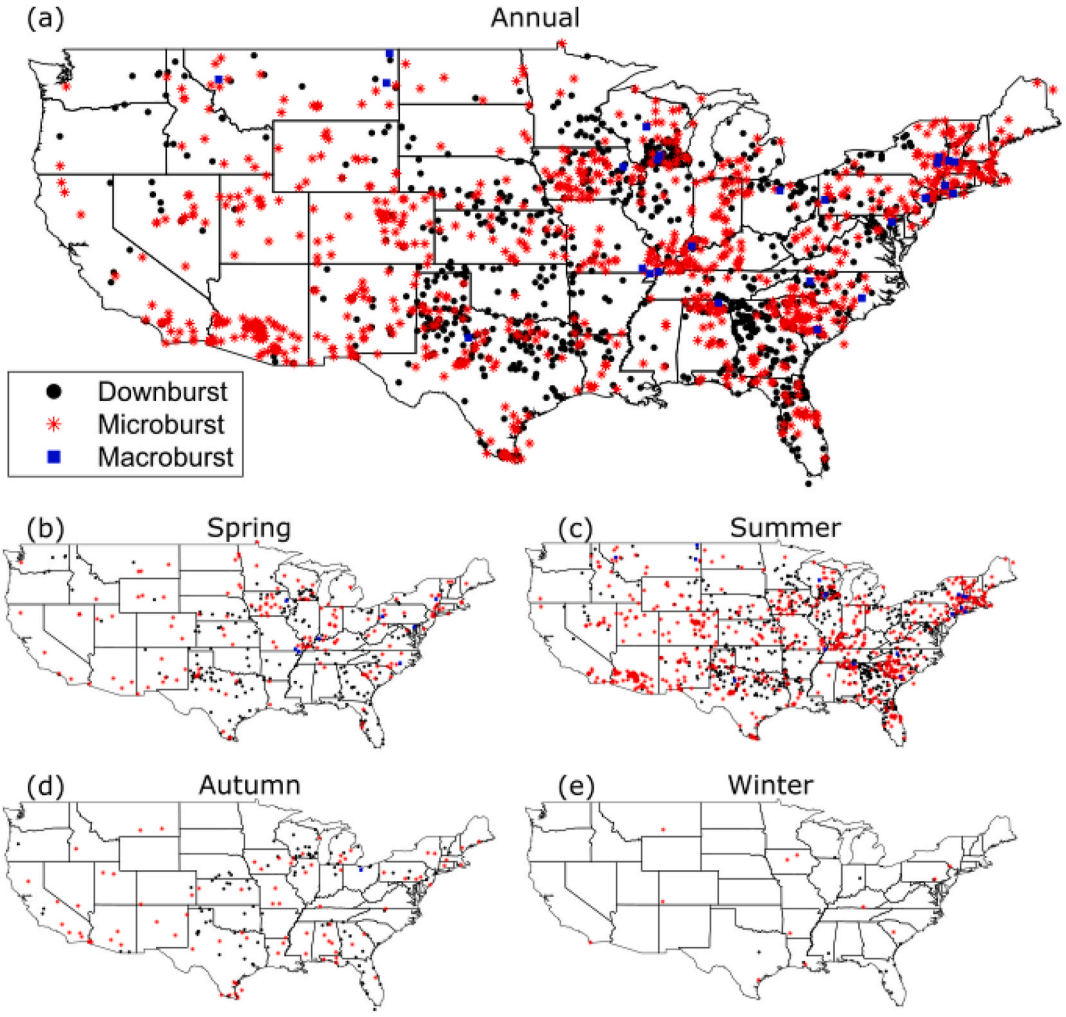

Fig. 1. Spatial distribution of downburst events with division into downbursts, microbursts and macrobursts (as indicated in the severe weather report description) over the years 2000–2019.

Table 2
Best discriminators between nonsevere and downburst-producing thunderstorms ranked on AUC (area under receiver operating characteristic curve) value. Following abbreviations are used: LR - lapse rate, SB - surface based, ML - mixed-layer, RH - relative humidity. TSTM stands for a thunderstorm.

	Variable	Units	Mean (non-severe TSTM)	Mean (downburst)	AUC
1	Downburst Environment Index	unitless	−0.71	0.11	0.714
2	Cold Pool Strength	°C	6.96	9.99	0.674
3	LR 0–4 km	K km^{-1}	6.02	6.55	0.673
4	LR 0–3 km	K km^{-1}	5.95	6.67	0.669
5	WINDEX	unitless	13.27	19.65	0.662
6	LR 0–2 km	K km^{-1}	5.70	6.80	0.661
7	T2M	°C	22.28	26.14	0.659
8	LR 0–6 km	K km^{-1}	6.02	6.27	0.658
9	SB LCL	m AGL	784.37	948.86	0.654
10	ML LCL	m AGL	1022.54	1133.45	0.645
11	LR 0–1 km	K km^{-1}	5.36	6.96	0.640
12	DCAPE	J kg^{-1}	530.07	631.23	0.629
13	LR 0–500m	K km^{-1}	5.50	7.30	0.624
14	WMAXSHEAR	m^2 s^{-2}	328.86	513.58	0.617
15	Delta Theta-E	°C	7.77	13.94	0.607
16	Derecho Composite Parameter	unitless	0.40	0.75	0.604
17	Mean RH 0–2 km	%	0.74	0.65	0.602
18	SB Lifted Index	°C	−1.21	−3.43	0.601
19	Energy Helicity Index 0–3 km	unitless	0.36	0.61	0.593
20	ML CAPE	J kg^{-1}	907.96	1294.41	0.582

sources outside the NWS. These include but are not limited to the media, law enforcement and other government agencies, emergency managers, private companies, individuals, etc. (NWS 2021). While the NWP attempts to verify all reports that are provided from sources outside of the NWP, information from these sources may sometimes be unverified by the NWS due to limited time, personnel and resources. Therefore, there is no guarantee on the accuracy or validity of the provided information. The reports are the so-called "as is" data.

To evaluate atmospheric environment associated with downburst events and construct background climatology we use recently released 5th generation of ECMWF reanalysis (ERA5; Hersbach and Coauthors, 2020). In this reanalysis, significant improvements in vertical (137 model levels), spatial (0.25° grid) and temporal (1-h step) resolution have been introduced compared to prior global reanalyses such as ERA-Interim (Dee and Coauthors, 2011), MERRA2 (Gelaro et al., 2017), CFSR (Saha et al., 2014) or NCEP/NCAR (Kistler et al., 2011). In this study, we use terrain-following hybrid-sigma model levels to compute convective parameters as these levels are more accurate compared to less numerous pressure levels, especially considering a boundary-layer. For each raw ERA5 vertical profile we consider temperature, humidity, pressure, geopotential, *U* and *V* wind components and process them using *thundeR* R language package (Taszarek et al., 2021). Mixed-layer (ML) parcel is defined based on mixing the layer of 0–500 m above ground level (AGL). Downdraft-related metrics such as DCAPE or cold pool strength are computed by defining a mean theta-e in 3–5 km AGL layer and using it to bring a parcel along moist adiabat from 4 km AGL down to the surface. For all parcel computations a virtual temperature correction is applied (Doswell and Rasmussen 1994). Many parameters used in this study are based on the parcel theory which assumes that (1) the pressure inside the parcel is always the same as the ambient hydrostatic pressure; (2) parcel's trajectory is vertical and there is no vertical motion that compensate for the parcel's descent; and (3) the process is adiabatic and the parcel does not mix with the surrounding atmosphere. Gilmore and Wicker (1998) demonstrated using numerical models that these three assumptions are always violated to some extent in severe convective storm environments. For example, downdrafts are not purely vertical but inclined due to the cloud translation and the interaction with background winds (Romanic and Hangan 2020). Similarly, the nonhydrostatic contributions to pressure fields are often significant in convective environments. Therefore, results should be always interpreted with caution as these metrics represent certain limitations in sampling convective environments. While convective parameters derived from ERA5 reanalysis compare favorably to sounding data across the U. S., larger errors can be found for boundary-layer parameters with underestimation of CAPE, low-level moisture, and wind shear, particularly when considering extreme values (Li et al., 2020; Taszarek et al., 2021).

In addition, we also use lightning data from the National Lightning Detection Network (NLDN; Cummins and Murphy 2009; Kingfield et al., 2017; Koehler 2020) in constructing climatology as a filter to focus only on those ERA5 environments that resulted in convective initiation. We use all cloud-to-ground lightning events gridded to 0.25° boxes with 1-h temporal steps to match resolution of ERA5. Only situations with at least 2 lightning flash detections per grid per hour are considered as the initiating environment. Consistent with dataset used in Taszarek et al. (2020b), we use the same NLDN and severe weather reports datasets to create a nonsevere thunderstorm category, i.e., situations with detected lightning, but no severe hail, tornado or wind report within a diameter of 45 km and ±3-h. We use this category as null cases to evaluate how nonsevere thunderstorm environment differs from those that lead to downburst events. In total, 1,121,466 unique ERA5 profiles for nonsevere thunderstorms, 927 for downbursts, 914 for microbursts and 27 for macrobursts (consistent with the name used in Storm Events Database reports) are evaluated in this study. In analyzing convective environments we consider all three categories as one downburst category to account for limited sample size. Climatology maps for ERA5 and NLDN are constructed for the period 1989–2019.

3. Results and discussion

3.1. Issues with downburst reports

The locations of all identified downburst-like winds across the continental U.S. is provided in Fig. 1. These wind systems are more frequent in the central and southeastern part of the U.S. than the rest of the country, which is likely affected by the climatological frequency of thunderstorms itself (Koehler 2020; Taszarek et al., 2020a). Most of the downburst events were reported during summer and spring. We also observe a significant spatial variability of reported downbursts that is unlikely to be a result of natural processes, but rather artificially caused by the population density. A good example of artificial influence on the spatial pattern of observations is the abrupt discontinuity in the number of observed microbursts between southern and northern Arizona, especially considering Phoenix metropolitan area (Fig. 1). Northern Arizona and southern Utah are significantly less populated than southern Arizona and these population differences are further reflected in the apparent absence of downbursts over north Arizona. However, a large contrast in elevation should be also noted as a contributing factor. A similar observation holds for the reported lack of downbursts in central Texas along the zonal stripe between Dallas to the north and Austin, San Antonio and Houston to the south (Fig. 1). This result is consistent with prior studies where a large bias between severe weather reports from Storm Events Database and population density was also found (Edwards et al., 2018; Potvin et al., 2019; Taszarek et al., 2020a; Gensini et al., 2020).

One of the reasons for the observed inhomogeneity of the downburst and microburst reports could be the inconsistency in the reporting standards between different forecasting offices (Doswell et al., 2005). For example, nearly all events in Alabama, Colorado and Utah are microbursts, which suggests that their offices tend to classify all such events as microbursts. The opposite observation holds for Oklahoma and Arkansas where the majority of the reported events are classified as downbursts. More diversity in the separation between downbursts and microbursts is found in northern Kansas and southern Nebraska. In terms

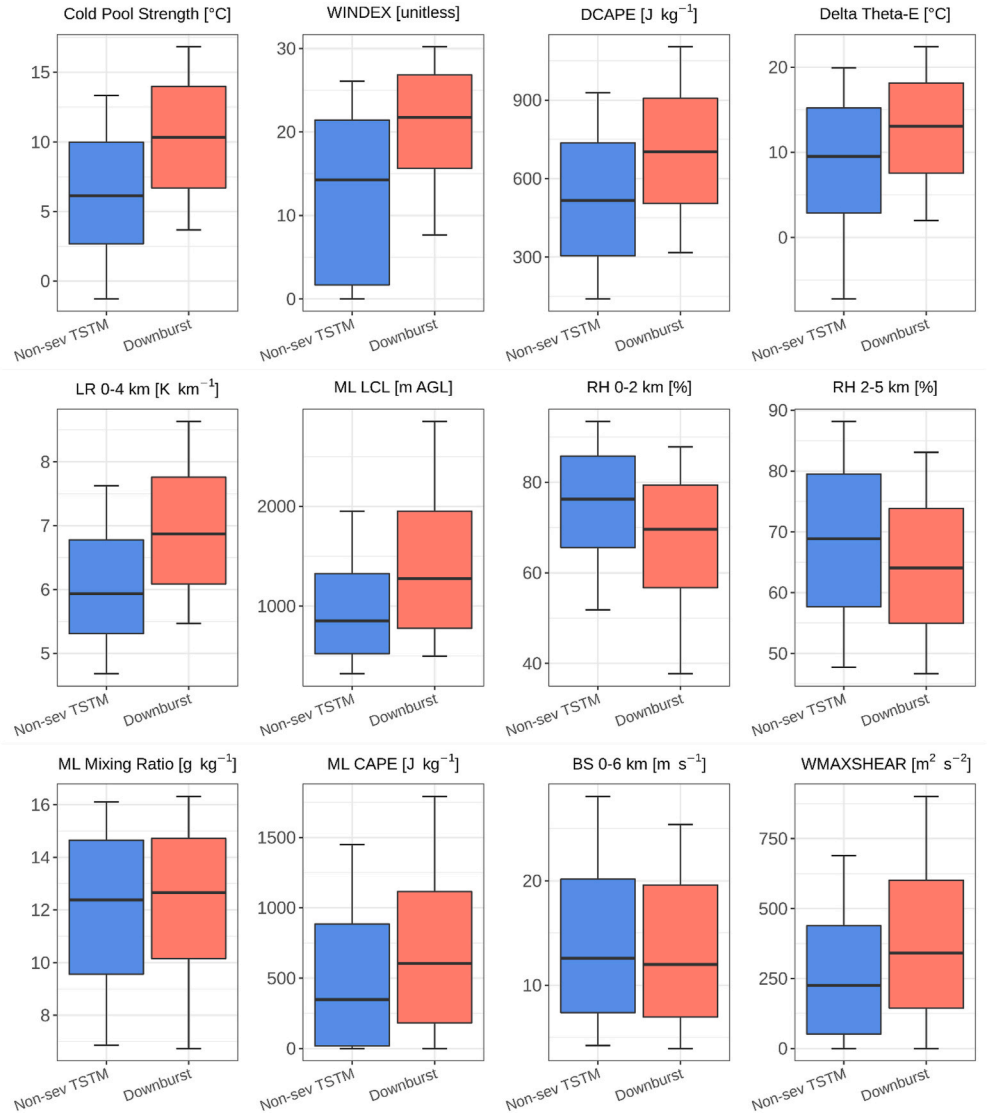

Fig. 2. Box-and-whisker plots of selected convective parameters for nonsevere (blue) and downburst-producing (red) thunderstorms. The median is represented as a horizontal line inside the box, the edges of the box represent the 25th and 75th percentiles, and whiskers represent the 10th and 90th percentiles. Convective variables are derived from ERA5 proximity grid points. (For interpretation of the references to colour in this figure legend, the reader is referred to the Web version of this article.)

of natural factors that could have contributed to this discrepancy in reported type of downburst-like winds, Kingsmill and Wakimoto (1991) and Miller and Mote (2018) showed that the storm modes for the regions around Alabama, Colorado and Utah are usually associated with single-cells, multicells and pulse storms. On the other hand, the storms over Oklahoma and Arkansas are typically supercells, multicells or quasi-linear convective systems (Smith et al., 2013).

Further investigation of the number of reported microbursts and macrobursts in the Storm Events Database indicates that only ~3% of all downbursts across the U.S. are macrobursts and almost all downbursts (~97%) are microbursts. This large discrepancy in the reported occurrence of these two downburst subcategories suggests there is a systematic bias in reporting microbursts over macrobursts. The bias towards reporting microbursts over macrobursts can also be inferred from media reports as well as scientific literature (e.g., Miller et al., 2020; Abbasi et al., 2021) that often tag all downburst-like winds as microbursts without further investigating the horizontal dimensions of the outflow.

3.2. Favorable downburst environments

At the first stage of environmental analysis, we evaluated distributions of 172 thermodynamic, kinematic and composite atmospheric parameters for nonsevere and downburst-producing thunderstorm events (downbursts, microbursts and macrobursts combined into one category to account for limited sample size). All parameters were then ranked based on their ability in discriminating between nonsevere and downburst categories. For this purpose, we used categorical data to calculate receiver operating characteristic (ROC; Mandrekar 2010) curves and area under the curve (AUC; Mandrekar 2010). In the first step we combined all available downburst reports (true) with a random sampling of 10,000 nonsevere thunderstorm events (false), performed ROC and AUC calculations, and then repeated this process again 1000 times, each with a different random sampling. We did this because nonsevere thunderstorm category sample size of >1 million profiles is much larger compared to downburst reports that are also likely highly underreported and spatially biased (see Section 3a). Finally, we calculated the mean ROC and AUC from all iterations and used them to rank convective parameters. We use this methodology as it has been commonly applied in the field of atmospheric sciences in the forecast/model verification, and it provides robust results regarding skill of certain parameters along their full percentile distribution. In Table 2 we present 20 best performers based on mean AUC values. Moderate AUC values indicate that forecasting and studying downburst environments is a very challenging task as most of the parameters do not show a skillful discrimination between nonsevere and downburst-producing environments.

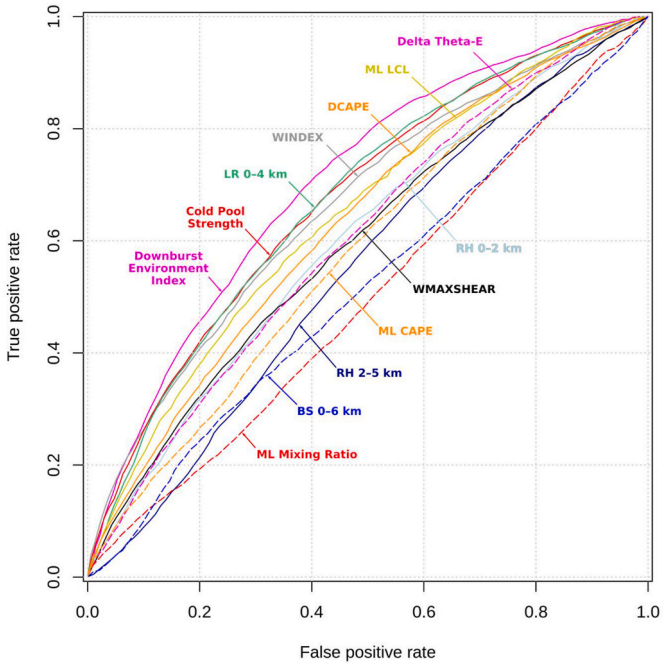

Fig. 3. Receiver operating characteristic curves calculated for selected convective parameters (as in Fig. 2) for nonsevere (false) and downburst-producing (true) thunderstorms.

As presented in Table 2 and Fig. 2, cold pool strength (difference in ambient temperature and the downdraft at the surface) turned out to be the most skillful parameter, followed by low-level temperature lapse rates and WINDEX (McCann 1994). Other useful metrics included also lifted condensation level, 2-m temperature, DCAPE, WMAXSHEAR (a square root of two times ML CAPE multiplied by 0–6 km wind shear; Taszarek et al., 2020b), delta theta-e (difference in theta-e between mean 3–5 km and the surface), derecho composite parameter (Evans and Doswell 2001) and mean low-level relative humidity. For comparison, we also show in Figs. 2 and 3 that parameters commonly used in the operational forecasting of convective storms such as ML mixing ratio or 0–6 km wind shear (BS 0–6 km) turned out to be not very skillful in discriminating between nonsevere and downburst-producing thunderstorms as a standalone parameter. Our results also indicate that mean relative humidity at the lowest 2 km of the troposphere is more important than the mean value between 2 and 5 km (Figs. 2 and 3).

As many of the best performing metrics presented in Table 2 are heavily correlated with each other, in Table 3 we provide a Pearson correlation coefficient matrix combining selected most skillful parameters. Cold pool strength, which was defined as the best standalone downburst predictor, is well correlated with temperature lapse rate parameters, WINDEX, 2-m temperature, lifted condensation level, delta theta-e and the mean relative humidity. The lowest correlation of 0.10 for cold pool strength was achieved by combining it with WMAXSHEAR, which means that although both of these metrics demonstrate skill in identifying favorable downburst environments, they account for differing environmental conditions. This relationship is further explored by combining these two parameters on the x and y coordinate system to display a frequency of lightning and downburst events (Fig. 4a), and estimate conditional probability for the downburst occurrence given lightning (Fig. 4b). This probability is defined by dividing smoothed grids of downbursts frequency with smoothed grids of lightning frequency, which indicate the fraction of lightning events leading to downburst events. As indicated in Fig. 4b, probability for downburst increases along with increasing values of both cold pool strength and WMAXSHEAR. Using this dependence, we derive a linear function, so the slope of the function is parallel to the changes in downburst probability as presented in Fig. 4b. Position of this linear function is then defined by the equation, which we hereafter call a downburst environment index (DEI). The DEI is defined as:

$$DEI = \frac{1560 - (CPS - 13) + 13WXS}{10000} \quad (1)$$

where CPS is the cold pool strength [°C] and WXS is the WMAXSHEAR [$m^2\ s^{-2}$]. If WXS equals 0 $m^2\ s^{-2}$, then DEI is −2. If DEI is < −2 then it equals −2, which means the environment is unfavorable to downbursts. Values of DEI are scaled in the way that around 1 and 99th percentile of the downburst events in our dataset ranges from −2 to 2 respectively (Fig. 4c). Values exceeding 0 indicate a favorable downburst environment with a share of nonsevere thunderstorm situations decreasing along with increasing DEI. Although we are aware that limited sample size and the quality of downburst reports does not allow derivation of highly skillful estimates, a clear signal of increasing downburst conditional probabilities can be found in the phase space of cold pool strength and WMAXSHEAR. These two combined in the form of DEI outperformed all other available metrics evaluated in this work (Table 2, Fig. 3). Considering how challenging and difficult it is to study and forecast downbursts, AUC of 0.71 obtained for DEI offers a promising opportunity to evaluate climatological aspects of favorable downburst environments. However, due to still limited skill, results should be interpreted with caution as not every favorable downburst environment will result in a development of actual downburst. Future research with a larger sample of reported downbursts should also reevaluate the performances of DEI and whether or not one parameter is sufficient to represent all downburst environments given that some downbursts are primarily thermodynamically and some are dynamically driven. In this context, machine learning models might be a promising way forward because they allow encapsulation of multiple processes rather than the fixed parameter approach, provided they are appropriately trained (McGovern et al., 2019).

Table 3
Pearson correlation coefficient matrix for selected best downburst predictors (see Table 2).

	Cold Pool Strength	LR 0–4 km	WINDEX	T2M	ML LCL	DCAPE	WMAXSHEAR	Energy Helicity Index 0–3 km	RH 0–2 km	Delta Theta-E	ML CAPE
Cold Pool Strength	**X**	0.90	0.88	0.89	0.77	0.75	0.10	0.12	−0.68	0.70	0.40
LR 0–4 km	0.90	**X**	0.81	0.70	0.83	0.54	0.01	0.01	−0.73	0.44	0.19
WINDEX	0.88	0.81	**X**	0.85	0.67	0.54	0.05	0.11	−0.54	0.62	0.45
T2M	0.89	0.70	0.85	**X**	0.63	0.62	0.04	0.12	−0.52	0.69	0.44
ML LCL	0.77	0.83	0.67	0.63	**X**	0.63	−0.18	−0.09	−0.87	0.16	−0.04
DCAPE	0.75	0.54	0.54	0.62	0.63	**X**	0.25	0.26	−0.68	0.59	0.43
WMAXSHEAR	0.10	0.01	0.05	0.04	−0.18	0.25	**X**	0.65	0.04	0.39	0.53
Energy Helicity Index 0–3 km	0.12	0.01	0.11	0.12	−0.09	0.26	0.65	**X**	−0.02	0.36	0.53
RH 0–2 km	−0.68	−0.73	−0.54	−0.52	−0.87	−0.68	0.04	−0.02	**X**	−0.20	−0.04
Delta Theta-E	0.70	0.44	0.62	0.69	0.16	0.59	0.39	0.36	−0.20	**X**	0.73
ML CAPE	0.40	0.19	0.45	0.44	−0.04	0.43	0.53	0.53	−0.04	0.73	**X**

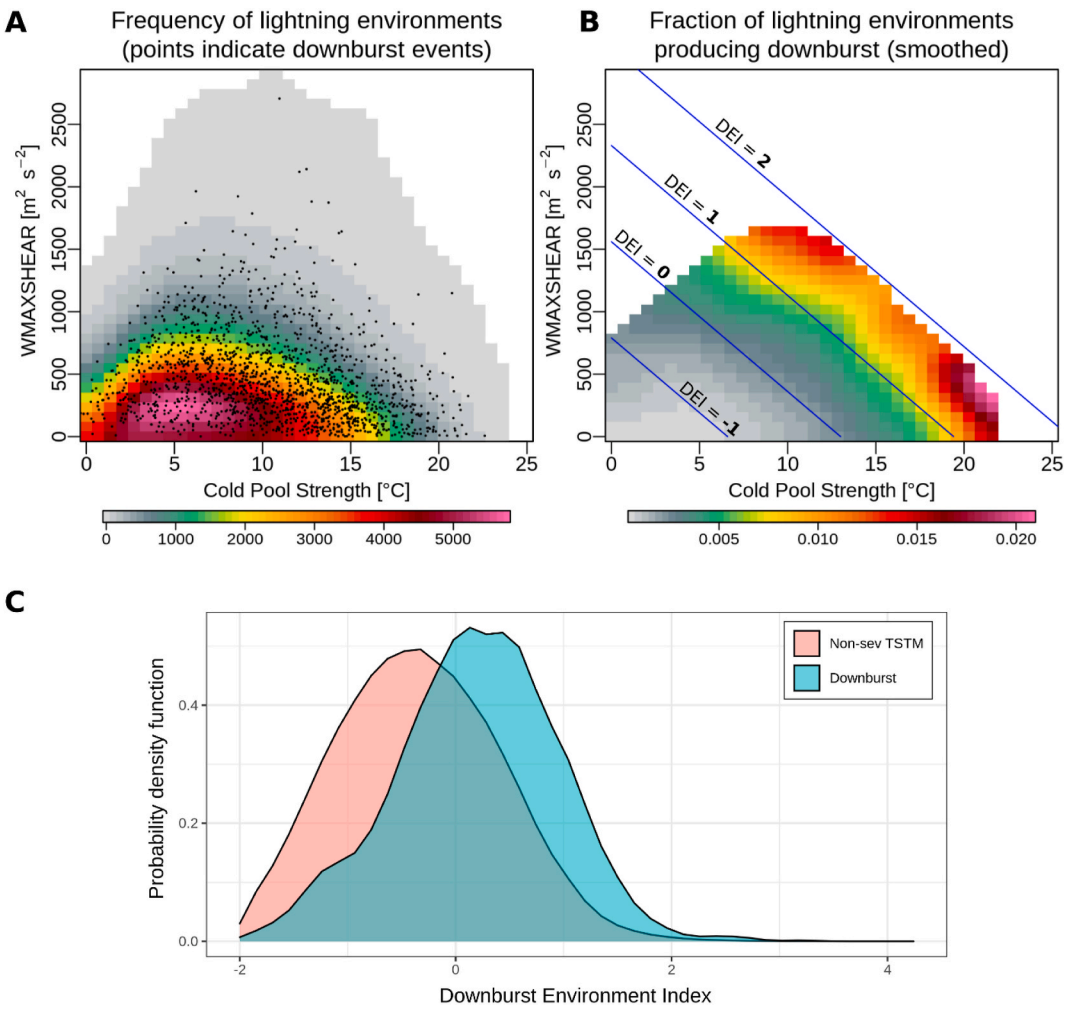

Fig. 4. Climatological frequency of environments with detected lightning (shaded) with downburst events indicated as black points (a), conditional probability for downburst occurrence given lightning (b), and probability density functions of nonsevere and downburst-producing thunderstorms for downburst environment index (values ≤ -2 are excluded) (c). A 5 × 5 grid focal mean smoothing was applied to (a) and (b).

3.3. Climatological aspects of favorable downburst environments

In this section, a climatological frequency of favorable downburst environments using a previously formulated DEI parameter is evaluated. We firstly focus on a mean annual frequency (hours) of DEI >0 environments in ERA5 both unfiltered and filtered with detected lightning from the NLDN network. Then, we turn our attention to the most extreme and rare environments consisting of the 99th percentile of DEI to show where environmental potential for downburst is the highest. All metrics are considered over meteorological seasons.

In agreement with downburst reports (Fig. 1.), favorable downburst environments are the most frequent during summer, then spring, autumn and winter. During spring, favorable environments are observed over southern portions of the Great Plains and parts of Southeast including Florida (Fig. 5), both with and without applied lightning filters. During summer, favorable downburst environments can develop in any part of the country, but a clear peak in their frequency is observed over the southern Great Plains. This area is however heavily capped with considerable amounts of convective inhibition (Gensini et al., 2011) and thus only a small fraction of these environments results in convective development. For this reason, summertime favorable downburst environments filtered with lightning are the most frequent over Southeast, Florida, High Plains and southwest U.S. where storms are driven by the North American monsoon (Adams and Comrie 1997). However, due to formulation of a DEI parameter, our estimates may have a bias toward thermodynamically driven downbursts. This may lead to neglecting dynamic contributions in downbursts produced by the mesoscale convective systems that frequent the Northern Plains and the Midwest. In the High Plains and Southwest, strong downburst winds are usually produced from negative buoyancy primarily caused by evaporation of raindrops, and melting and sublimation of ice (Wakimoto 1985). On the other hand, downbursts in the southeastern U.S. are associated with the clouds that have a shallower and warmer base than the clouds over the High Plains (Atkins and Wakimoto 1991). In the latter case, the subcloud environment is more stable. The former environments are characterized by the vertical profile that is closer to a dry adiabatic lapse rate and the constant mixing ratio between the surface and 500 mb (Wakimoto 1985), whereas the latter atmosphere is usually moist adiabatic (Fujita 1983; Atkins and Wakimoto 1991; Burlando and Romanic 2020). Storms over High Plains and Southwest are characterized by steep low-level lapse rates, low relative humidity and thus high values of cold pool strength and DCAPE favoring dry microburst type winds while storms over Southeast are characterized by high relative humidity and CAPE, heavy hydrometeor loading of the updraft, and thus are driven by a wet downburst type winds.

During autumn and winter a significant drop in the frequency of favorable downburst environments can be observed with most of the activity limited mainly to southern parts of the U.S.. As the spatial patterns over seasons are obviously driven by the overall frequency of lightning, we also evaluate which fraction of total lightning hours is

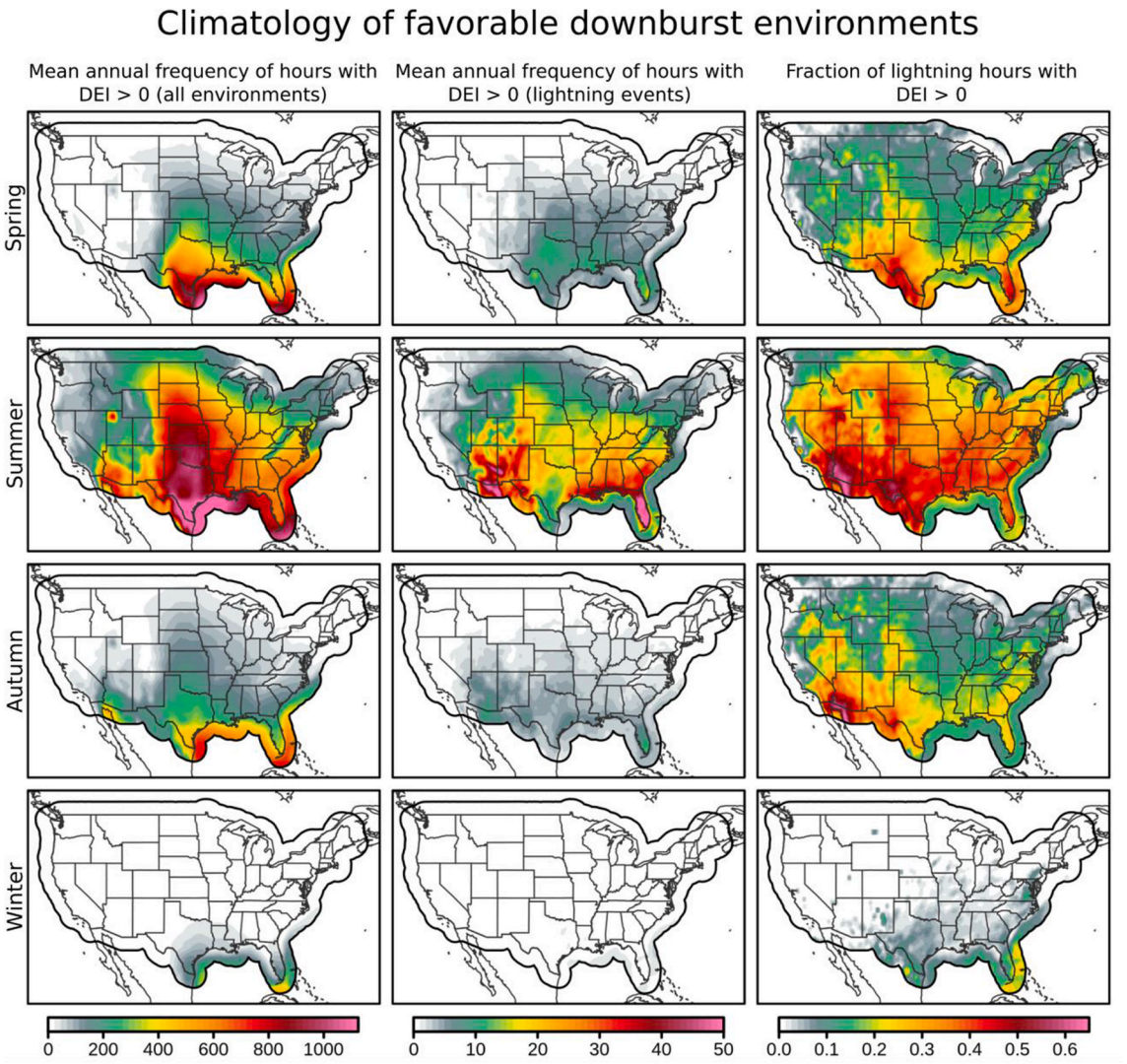

Fig. 5. Mean annual frequency of hours with Downburst Environment Index (DEI) > 0 (see Fig. 4) over seasons (rows) considering all available environments (first column), and only hours with detected lightning (middle column). A fraction of hours with DEI >0 among all hours with detected lightning is indicated in a third column. Based on a period of 1989–2019, ERA5 reanalysis, and NLDN lightning data. Black line indicates the area for which NLDN was available.

associated with favorable downburst environments (Fig. 5). In every season except winter, the highest fractions are observed over southern Great Plains and southwest (0.3–0.6) whereas the lowest are across Midwest (0.1–0.3). During summer and autumn, any storm developing over southwest has approximately 50% probability that it will be supported by an environment favorable for downbursts. The proxy of DEI >0 with lightning filter identifies the region of Arizona as prone to severe thunderstorm winds during summer, which is further in accordance with the high frequency of reported microbursts in that area (Fig. 1).

Evaluation of the most extreme and rare downburst environments defined by the 99th percentile of DEI (Fig. 6), indicate that the area along the Great Plains is the most vulnerable to such situations (DEI >2.5). During spring peak, DEI values are observed over southern Great Plains (consistent with frequency of favorable downburst environments; Fig. 5) while during summer they move towards northern Great Plains and reach overall the highest values (Fig. 6). If we consider only environments with detected lightning a contrasting pattern can be observed during summer when the most extreme DEI environments are compared with the frequency of DEI >0. While the most extreme downburst environments occur along the Great Plains, the highest frequency of favorable environments is over Southwest and Southeast (Figs. 5 and 6). During Autumn potential for extreme downburst environments drops with 99th percentile of DEI typically not exceeding 1.5, while during winter a fairly low potential is limited mainly to Southern Great Plains and Southeast (Fig. 6).

As our downburst reports are only from the land surface, climatological results should be applied primarily to the land surface only. Differences among land and water surface found i n Figs. 5 and 6 are mainly driven by differing climatological patterns in lightning frequency and thermodynamic instability which during summer is higher over the land surface, while during winter over the water. Cheng et al. (2021) also indicated that instability behaves differently as an environmental lightning proxy over the ocean compared to the land.

3.4. Vertical profiles of theta-e

The vertical profiles of normalized theta-e for all documented downburst-like events in the Storm Events Database over Alabama (52 events), Florida (92), Oklahoma (25), and Illinois (42) are shown in Fig. 7. In respective order, field measurement campaigns MIST (Atkins and Wakimoto 1991), FACE (Caracena and Maier 1987), NSSL (Eilts and Doviak 1987) and NIMROD (Fujita 1985) are included for comparison. The theta-e profiles from this study are the ensemble mean of individual theta-e profiles extracted from ERA5 for the closest grid point and

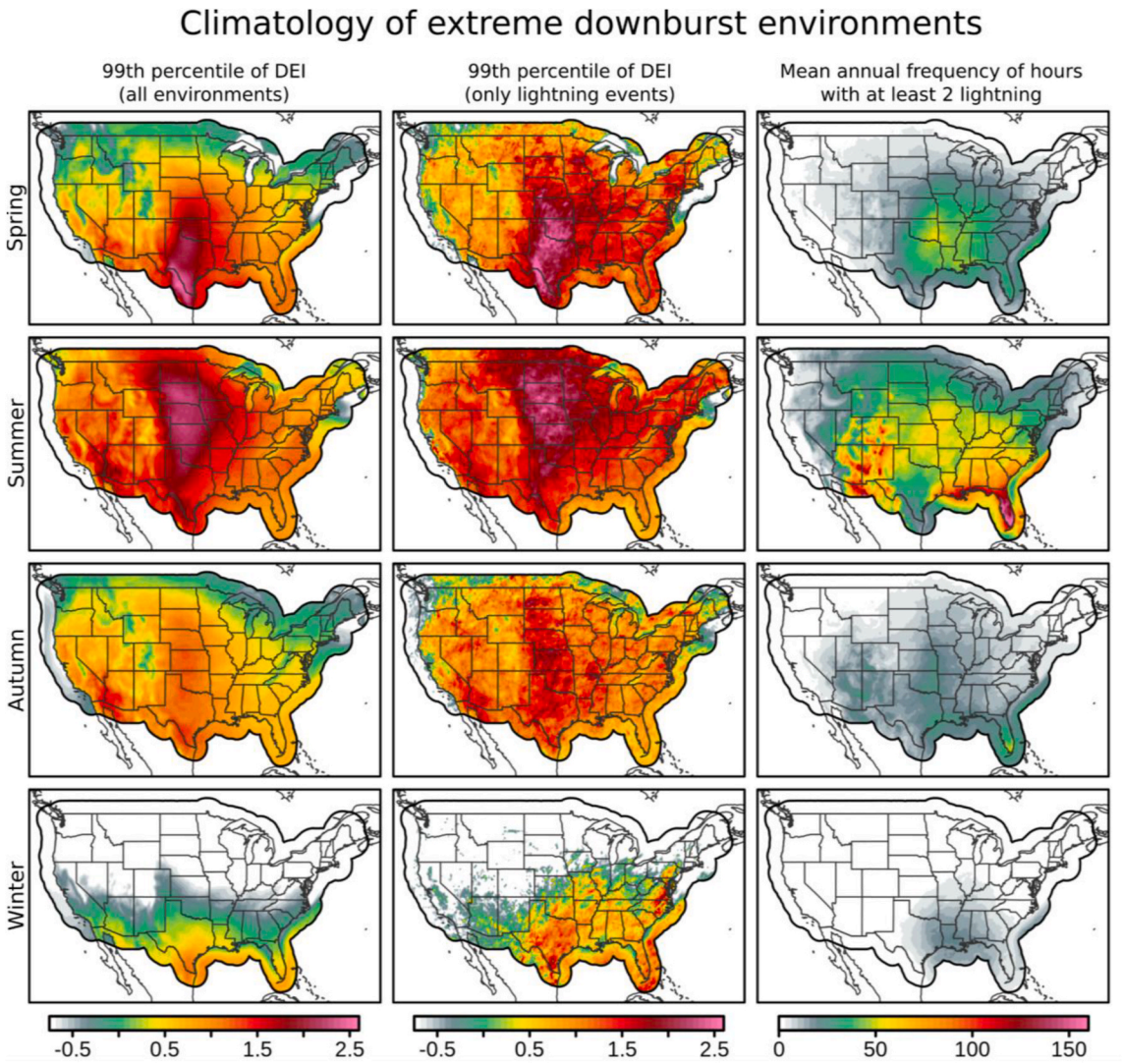

Fig. 6. 99th percentile of Downburst Environment Index (DEI) over seasons (rows) considering all available environments (first column), and only hours with detected lightning (middle column). Mean annual frequency of hours with at least 2 lightning is indicated in a third column. Based on a period of 1989–2019, ERA5 reanalysis, and NLDN lightning data. Black line indicates the area for which NLDN was available.

reanalysis timestep to the registered downburst events in the Storm Events Database. The reanalysis profiles are more similar to the field measurements in Alabama and Florida (i.e., coastal states) than they are in Oklahoma and Illinois (i.e., in-land states). Fig. 7 further shows that the mid-level values of theta-e are between 0.94 and 0.96 of the surface value. While working with absolute values that were shifted to the same surface value of theta-e rather than normalized profiles, Atkins and Wakimoto (1991) proposed that the difference of >13 °C (~0.95 of surface value) and particularly >20 °C (0.92 of surface value) between the surface and mid-level values of theta-e is a reliable indicator of microbursts in the afternoon. In both reanalysis profiles and field observations, minimum theta-e is found between 700 and 500 hPa. The consistent underestimations of minimum theta-e in the reanalysis profiles are not surprising given that the field measurements were specifically designed for downburst analysis and the radiosondes were released in the close proximity of clouds that produced downbursts. While the theta-e profiles from the JAWS campaign around Denver, Colorado (McCarthy et al., 1982) were not provided in literature, the reanalysis profiles (not shown) have shown that the mid-level theta-e is only 0.98 of the surface value.

Fig. 8 shows the profiles of theta-e for different types of downburst winds and nonsevere thunderstorm events over the entire U.S.. All wind event profiles resemble a very similar overall pattern with macrobursts having typically a lower value of theta-e in the mid-troposphere and microbursts having the highest. Downburst-type events are somehow between these two, but typically with the highest surface value of theta-e. However, it is interesting to note that at the level of 800 hPa all three types share almost identical values of theta-e. The minimum theta-e is typically at 600 hPa and ranges between 327 K (macrobursts) and 329 K (microbursts). There is a considerable difference between theta-e for nonsevere lightning cases and wind events at the lower troposphere, which indicates that this environmental characteristic is important in identifying a downburst potential. Further investigation indicates a rather minor difference in the low-level temperature profile and no considerable differences in the vertical profiles of dew points between nonsevere lightning and wind events (Fig. 8). Deviations are however noted for the macrobursts events for the wind speed, which is higher than in the other categories. This result may be however driven by the very small sample size of this category (only 27 cases), and the fact that the majority of these events were reported in the northern portions of the U.S. (Fig. 1), where from the climatological standpoint wind speed is typically higher (polar jet stream). It is also important to mention that ERA5 profiles (Fig. 9) are only a modeled approximation of real atmospheric conditions. and reanalyses are burdened with inaccuracies

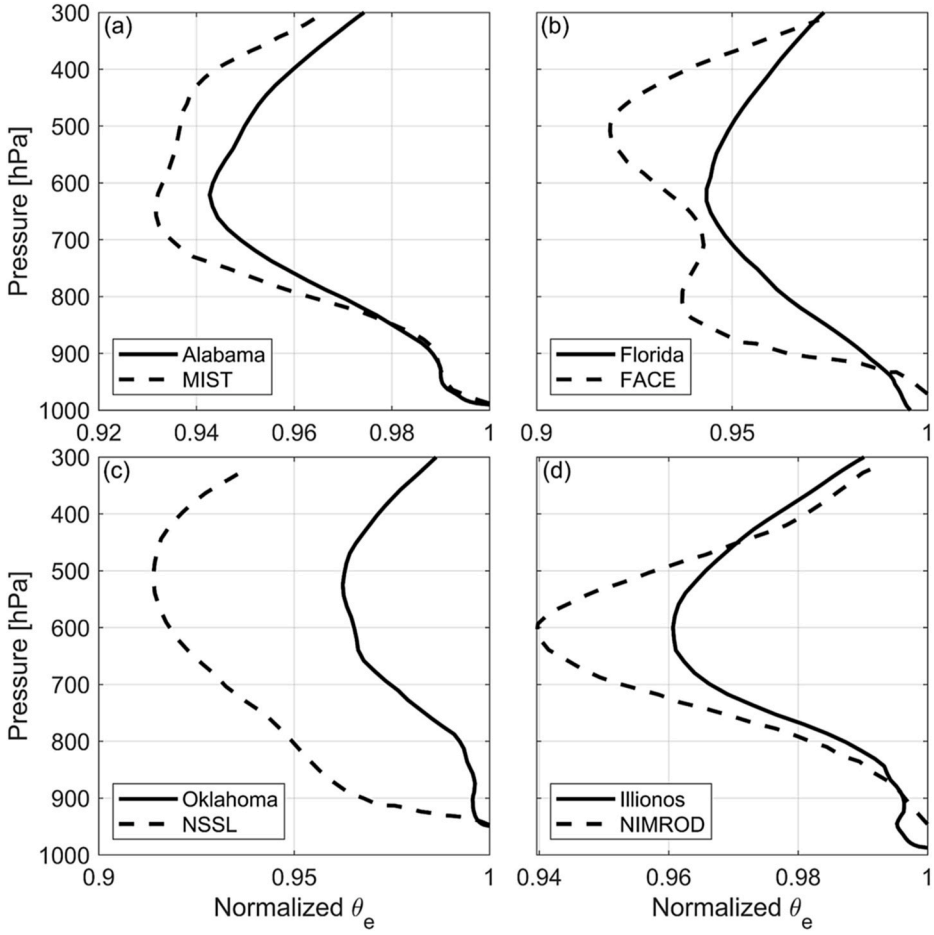

Fig. 7. (a) Vertical profiles of the normalized theta-e (θ_e) for all downburst events over (a) Alabama; (b) Florida; (c) Oklahoma; and (d) Illinois from reanalysis data (solid lines). Dashed lines in the subplots are the sounding data from the field measurements that were performed in these states. The references for field observations are provided in the text.

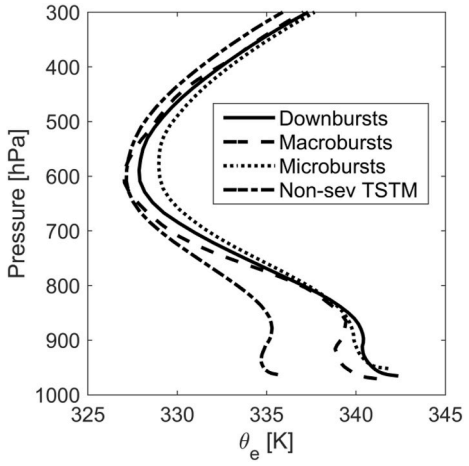

Fig. 8. Vertical profiles of theta-e (θ_e) for downbursts, macrobursts, microbursts and nonsevere thunderstorms.

resulting from parameterization schemes, data assimilation issues and convective contamination (Tippett et al., 2014; King and Kennedy 2019; Taszarek et al., 2021). For this reason, results should be always interpreted with caution.

4. Summary and concluding remarks

This paper tested the ability of convective parameters in representing downburst events and investigated the climatology of their favorable environments across the contiguous U.S.. The analyses were based on the Severe Weather Event Reports provided by the NCEI (in this paper referred to as Storm Events Database), the ECMWF ERA5 reanalysis and the lightning data from the National Lightning Detection Network (NLDN). The focus was first given to the systematic bias in microburst and macroburst reporting in the period January 2010–June 2020. Microbursts and macrobursts are downbursts with the radial extent of damaging winds below and over 4 km from the downdraft impact zone, respectively. During this period, only 27 macroburst events were reported in comparison to 914 microburst entries. Moreover, 927 severe wind events were classified as downbursts without further specifying the size of the outflow. We also found a spatial variability of reported downbursts that is unlikely to be a result of natural processes, but rather artificially caused by population density.

In environmental analysis by comparing nonsevere and downburst-producing storms we showed that cold pool strength, low-level lapse rates, WINDEX, lifted condensation level, DCAPE, WMAXSHEAR, derecho composite parameter, 2-m temperature, delta theta-e, and mean low-level relative humidity demonstrated some value as downburst predictors. However, many of the top performing metrics are heavily correlated with each other (e.g., low-level relative humidity and lifted condensation level). Therefore, by combining the best predictor (cold pool strength) with the least correlated WMAXSHEAR we created a

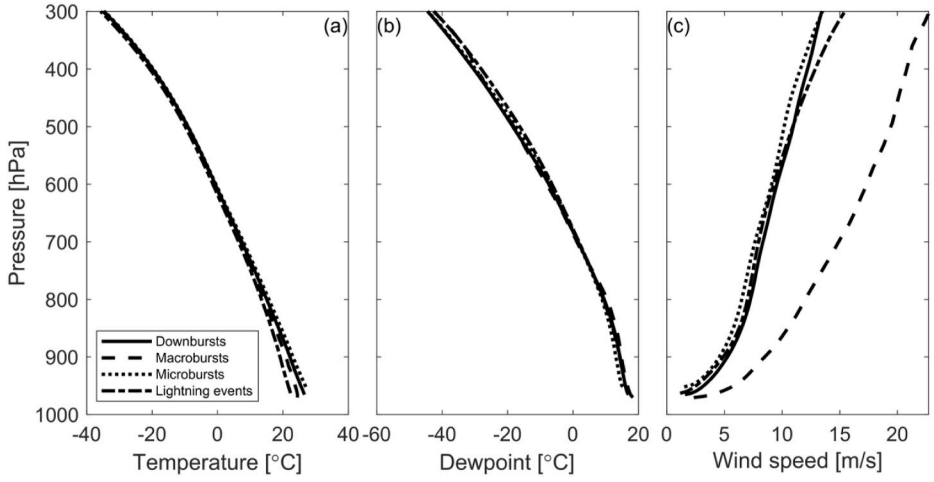

Fig. 9. Vertical profiles of temperature, dewpoint and wind speed for downbursts, macrobursts, microbursts and nonsevere thunderstorms.

downburst environment index (DEI) and used it to model climatological frequency of favorable downburst environments. Favorable environments conditioned on lightning are the most frequent during summer over Southwest and Southeast. The most extreme downburst environments defined by the 99th percentile of DEI occur exclusively along the Great Plains of the U.S. during spring and summer. Due to formulation of a DEI parameter, our estimates may have a bias toward thermodynamically driven downbursts. This may lead to neglecting dynamic contributions in downbursts produced by the mesoscale convective systems that frequent the Northern Plains and the Midwest (Haberlie and Ashley 2019).

While the frequency of favorable downburst environments follows the general climatological frequency of severe thunderstorms and their environments (Gensini and Ashley 2011; Smith et al., 2012; Gensini et al., 2020; Li et al., 2020; Taszarek et al., 2020a, 2020b), we found that some patterns of spatial variability of reported downburst events are likely affected by population density. For example, the Storm Events Database showed abrupt discontinuity in the number of observed microbursts between southern and northern Arizona. Given that northern Arizona and southern Utah are less populated than southern Arizona, we argued that these population differences are likely the cause of apparent absence of downbursts over northern Arizona, in addition to contrast in elevation. Similar patterns in the lack of reported downbursts were found in central Texas. The Storm Event Database also showed inconsistency in the labeling of downburst and microburst between different NWS forecasting offices. We demonstrated that nearly all events in Alabama, Colorado and Utah were labeled as microbursts, whereas almost all events were categorized as downbursts in Oklahoma and Arkansas.

The vertical profiles of theta-e for the reported downburst events extracted from the ERA5 reanalysis and four field campaigns yielded that the minimum value of theta-e was found typically between 700 and 500 hPa. The lowest values of theta-e in the mid-troposphere were found for macrobursts, then for downbursts and the highest for microbursts. Comparison of nonsevere and downburst-producing thunderstorms yielded those changes in theta-e in the lowest 200 hPa were the most important in identifying downburst-producing thunderstorms.

While many prior studies focused on severe thunderstorm environments across the U.S. with the special focus on tornadoes and large hail (e.g., Brooks et al., 2003; Grams et al., 2012; Allen et al., 2015; Coffer et al., 2019; Gutierrez and Kumjian 2021), only a few research elaborations covered the topic of downburst environments. Severe wind environments across the U.S. were typically studied without further division into different physical mechanisms leading to their development (e.g., Kuchera and Parker 2006; Brown and Dowdy 2021), which was the motivation in this study. Although our results regarding vertical profile of theta-e in downburst events are broadly consistent with Atkins and Wakimoto (1991), we introduced new findings by testing 172 convective parameters, and developed a new metric to identify favorable downburst environments based on the relationship between cold pool strength and WMAXSHEAR parameters. Using ERA5 and NLDN lightning data we then estimated climatological frequency of such environments. However, considering how challenging and difficult it is to study and forecast downbursts, and that not every favorable environment will result in a development of actual downburst, these estimates should be interpreted with caution. Future research with a larger sample of reported downbursts should reevaluate if one composite parameter is sufficient in forecasting all downburst types. In this context, machine learning models might be a promising way forward.

As the present literature on downburst events and their environments is still very limited, we believe that more focus should be placed on exploring this topic, especially in the context of a warming climate and potential future changes in the frequency of convective wind hazards. As shown in the recent study by Pilguj et al. (2022), DCAPE, low-level lapse rates and relative humidity has become more favorable for downbursts over the last 40 years, and we speculate that this trend will likely continue in future as well.

Data availability statement

ERA5 data (temperature, specific humidity, geopotential, pressure, *U* and *V* wind components) was downloaded from the European Centre for Medium-Range Weather Forecasts (ECMWF), Copernicus Climate Change Service (C3S) at Climate Data Store (https://cds.climate.copernicus.eu/). National Lightning Detection Network dataset was provided by NOAA National Severe Storms Laboratory and due to the proprietary nature of the data they cannot be made openly available. Contact lightning@ou.edu for usage information. United States severe weather reports are available at the National Center for Environmental Information Storm Events Database (https://www.ncdc.noaa.gov/stormevents/ftp.jsp).

Author statement

Djordje Romanic: Conceptualization, Methodology, Writing- Original draft preparation, Investigation, Writing- Reviewing and Editing, Validation, Funding acquisition, Project administration, Mateusz Taszarek.: Methodology, Data curation, Writing- Original draft preparation, Investigation, Formal analysis, Software, Validation Writing- Reviewing and Editing, Funding acquisition. Harold Brooks: Writing- Original draft preparation, Investigation, Writing- Reviewing and Editing, Resources.

Declaration of competing interest

The authors declare that they have no known competing financial interests or personal relationships that could have appeared to influence the work reported in this paper.

Acknowledgments

This research of the first author was supported in part by the Wares Innovation Fund, and the Natural Sciences and Engineering Research Council of Canada (NSERC) Discovery grant (grant no. NSERC RGPIN-2021-02651). The research of the second author was supported by the Polish National Science Center (grant no. 2020/39/D/ST10/00768). The reanalysis computations were performed in the Poznań Supercomputing and Networking Center (project no. 448). We are grateful to the NOAA National Severe Storms Laboratory for providing NLDN lightning data. We also thank the NOAA National Centers for Environmental Information on providing the Storm Events Database.

References

Abbasi, E., Etemadi, H., Smoak, J.M., Rousta, I., Olafsson, H., Baranowski, P., Krzyszczak, J., 2021. Investigation of atmospheric conditions associated with a storm surge in the south-west of Iran. Atmosphere 12, 1429. https://doi.org/10.3390/atmos12111429.

Adams, D.K., Comrie, A.C., 1997. The North American monsoon. Bull. Am. Meteorol. Soc. 78, 2197–2213. https://doi.org/10.1175/1520-0477(1997)078<2197:TNAM>2.0.CO;2.

Allen, J.T., Tippett, M., Sobel, A., 2015. An empirical model relating United States monthly hail occurrence to large-scale meteorological environment. J. Adv. Model. Earth Syst. 7, 226–243. https://doi.org/10.1002/2014MS000397.

Atkins, N.T., Wakimoto, R.M., 1991. Wet microburst activity over the Southeastern United States: implications for forecasting. Weather Forecast. 6, 470–482. https://doi.org/10.1175/1520-0434(1991)006<0470:WMAOTS>2.0.CO;2.

Brooks, H.E., Lee, J.W., Craven, J.P., 2003. The spatial distribution of severe thunderstorm and tornado environments from global reanalysis data. Atmos. Res. 67–68, 73–94. https://doi.org/10.1016/S0169-8095(03)00045-0.

Brown, A., Dowdy, A., 2021. Severe convection-related winds in Australia and their associated environments. JSHESS. https://doi.org/10.1071/ES19052.

Burlando, M., Romanic, D., 2020. Groundbreaking contributions to downburst monitoring, modeling, and detection. In: Hangan, H., Kareem, A. (Eds.), The Oxford Handbook of Non-synoptic Wind Storms. Oxford University Press. Physical Sciences.

Caracena, F., Maier, M.W., 1987. Analysis of a microburst in the FACE meteorological mesonetwork in Southern Florida. Mon. Weather Rev. 115, 969–985. https://doi.org/10.1175/1520-0493(1987)115<0969:AOAMIT>2.0.CO;2.

Changnon, S.A., 2001. Damaging thunderstorm activity in the United States. Bull. Am. Meteorol. Soc. 82, 597–608. https://doi.org/10.1175/1520-0477(2001)082<0597:DTAITU>2.3.CO;2.

Cheng, W.Y., Kim, D., Holzworth, R.H., 2021. CAPE threshold for lightning over the tropical ocean. J. Geophys. Res. Atmos. 126, e2021JD035621 https://doi.org/10.1029/2021JD035621.

Childs, S.J., Schumacher, R.S., Adams-Selin, R.D., 2021. High-resolution observations of a destructive macroburst. Mon. Weather Rev. 149, 2875–2896. https://doi.org/10.1175/MWR-D-20-0412.1.

Cummins, K.L., Murphy, M.J., 2009. An overview of lightning locating systems: history, techniques, and data uses, with an in-depth look at the U.S. NLDN. IEEE Trans. Electromagn C. 51, 499–518. https://doi.org/10.1109/TEMC.2009.2023450.

Coffer, B.E., Parker, M.D., Thompson, R.L., Smith, B.T., Jewell, R.E., 2019. Using near-ground storm relative helicity in supercell tornado forecasting. Weather Forecast. 34, 1417–1435. https://doi.org/10.1175/WAF-D-19-0115.1.

Dee, D.P., Coauthors, 2011. The ERA-Interim reanalysis: configuration and performance of the data assimilation system. Q. J. R. Meteorol. Soc. 137, 553–597. https://doi.org/10.1002/qj.828.

Doswell, C.A., Rasmussen, E.N., 1994. The effect of neglecting the virtual temperature correction on CAPE calculations. Weather Forecast. 9, 625–629. https://doi.org/10.1175/1520-0434(1994)009<0625:TEONTV>2.0.CO;2.

Doswell, C.A., Rasmussen, E.N., Brooks, H.E., Kay, M.P., 2005. Climatological estimates of daily local nontornadic severe thunderstorm probability for the United States. Weather Forecast. 20, 577–595. https://doi.org/10.1175/WAF866.1.

Edwards, R., Allen, J.T., Carbin, G.W., 2018. Reliability and climatological impacts of convective wind estimations. J. Appl. Meteorol. Climatol. 57, 1825–1845. https://doi.org/10.1175/JAMC-D-17-0306.1.

Eilts, M.D., Doviak, R.J., 1987. Oklahoma downbursts and their asymmetry. J. Appl. Meteorol. Climatol. 26, 69–78. https://doi.org/10.1175/1520-0450(1987)026<0069:ODATA>2.0.CO;2.

Evans, J.S., Doswell, C.A., 2001. Examination of derecho environments using proximity soundings. Weather Forecast. 16, 329–342. https://doi.org/10.1175/1520-0434(2001)016<0329:EODEUP>2.0.CO;2.

Fujita, T.T., 1983. *Andrews AFB Microburst*. Satellite and Mesometeorology Research Project (SMRT). University of Chicago, p. 42. SMRT Research Report No. 205. https://swco-ir.tdl.org/handle/10605/262003.

Fujita, T.T., 1981. Tornadoes and downbursts in the context of generalized planetary scales. J. Atmos. Sci. 38, 1511–1534. https://doi.org/10.1175/1520-0469(1981)038<1511:TADITC>2.0.CO;2.

Fujita, T.T., 1985. *The Downburst: Microburst and Macroburst*. Satellite and Mesometeorology Research Project. Department of the Geophysical Sciences, University of Chicago, p. 136.

Gatzen, C., Fink, A.H., Schultz, D.M., Pinto, J.G., 2020. An 18-year climatology of derechos in Germany. Nat. Hazards Earth Syst. Sci. 20, 1335–1351. https://doi.org/10.5194/nhess-20-1335-2020.

Galway, J.G., 1989. The evolution of severe thunderstorm criteria within the weather service. Weather Forecast. 4, 585–592. https://doi.org/10.1175/1520-0434(1989)004<0585:TEOSTC>2.0.CO;2.

Geerts, B., 2001. Estimating downburst-related maximum surface wind speeds by means of proximity soundings in New South Wales, Australia. Weather Forecast. 16, 261–269. https://doi.org/10.1175/1520-0434(2001)016<0261:EDRMSW>2.0.CO;2.

Gelaro, R., Coauthors, 2017. The modern-era retrospective analysis for research and applications, version 2 (MERRA-2). J. Clim. 30, 5419–5454. https://doi.org/10.1175/JCLI-D-16-0758.1.

Gensini, V.A., Ashley, W.S., 2011. Climatology of potentially severe convective environments from the North American regional reanalysis. Electron. J. Severe Storms Meteor. 8. https://ejssm.org/ojs/index.php/ejssm/article/viewArticle/85.

Gensini, V.A., Haberlie, A.M., Marsh, P.T., 2020. Practically perfect hindcasts of severe convective storms. Bull. Am. Meteorol. Soc. 101, E1259–E1278. https://doi.org/10.1175/BAMS-D-19-0321.1.

Gilmore, M.S., Wicker, L.J., 1998. The influence of midtropospheric dryness on supercell morphology and evolution. Mon. Weather Rev. 126, 943–958. https://doi.org/10.1175/1520-0493(1998)126<0943:TIOMDO>2.0.CO;2.

Grams, J.S., Thompson, R.L., Snively, D.V., Prentice, J.A., Hodges, G.M., Reames, L.J., 2012. A climatology and comparison of parameters for significant tornado events in the United States. Weather Forecast. 27, 106–123. https://doi.org/10.1175/WAF-D-11-00008.1.

Gutierrez, R.E., Kumjian, M.R., 2021. Environmental and radar characteristics of gargantuan hail–producing storms. Mon. Weather Rev. 149 (8), 2523–2538. https://doi.org/10.1175/MWR-D-20-0298.1.

Haberlie, A.M., Ashley, W.S., 2019. A Radar-based climatology of mesoscale convective systems in the United States. J. Clim. 32, 1591–1606. https://doi.org/10.1175/JCLI-D-18-0559.1.

Hersbach, H., Coauthors, 2020. The ERA5 global reanalysis. Q. J. R. Meteorol. Soc. 146, 1999–2049. https://doi.org/10.1002/qj.3803.

Hjelmfelt, M.R., 1988. Structure and life cycle of microburst outflows observed in Colorado. J. Appl. Meteorol. 27, 900–927. https://doi.org/10.1175/1520-0450(1988)027<0900:SALCOM>2.0.CO;2.

James, R.P., Markowski, P.M., 2010. A numerical investigation of the effects of dry air aloft on deep convection. Mon. Weather Rev. 138, 140–161. https://doi.org/10.1175/2009MWR3018.1.

Kelly, D.L., Schaefer, J.T., Doswell, C.A., 1985. Climatology of nontornadic severe thunderstorm events in the United States. Mon. Weather Rev. 113, 1997–2014. https://doi.org/10.1175/1520-0493(1985)113<1997:CONSTE>2.0.CO;2.

King, A.T., Kennedy, A.D., 2019. North American supercell environments in atmospheric reanalysis and RUC-2. J. Appl. Meteorol. Climatol. 58, 71–92. https://doi.org/10.1175/JAMC-D-18-0015.1.

Kingfield, D.M., Calhoun, K.M., de Beurs, K.M., 2017. Antenna structures and cloud-to-ground lightning location: 1995–2015. Geophys. Res. Lett. 44, 5203–5212. https://doi.org/10.1002/2017GL073449.

Kingsmill, D.E., Wakimoto, R.M., 1991. Kinematic, dynamic, and thermodynamic analysis of a weakly sheared severe thunderstorm over Northern Alabama. Mon. Weather Rev. 119, 262–297. https://doi.org/10.1175/1520-0493(1991)119<0262:KDATAO>2.0.CO;2.

Kistler, R., Coauthors, 2001. The NCEP–NCAR 50–year reanalysis: monthly means CD–ROM and documentation. Bull. Am. Meteorol. Soc. 82, 247–267. https://doi.org/10.1175/1520-0477(2001)082<0247:TNNYRM>2.3.CO;2.

Knupp, K.R., 1989. Numerical simulation of low-level downdraft initiation within precipitating cumulonimbi: some preliminary results. Mon. Weather Rev. 117, 1517–1529. https://doi.org/10.1175/1520-0493(1989)117<1517:NSOLLD>2.0.CO;2.

Koehler, T.L., 2020. Cloud-to-ground lightning flash density and thunderstorm day distributions over the contiguous United States derived from NLDN measurements: 1993–2018. Mon. Weather Rev. 148, 313–332. https://doi.org/10.1175/MWR-D-19-0211.1.

Kuchera, E.L., Parker, M.D., 2006. Severe convective wind environments. Weather Forecast. 21, 595–612. https://doi.org/10.1175/WAF931.1.

Li, F., Chavas, D.R., Reed, K.A., Dawson II, D.T., 2020. Climatology of severe local storm environments and synoptic-scale features over North America in ERA5 reanalysis and CAM6 simulation. J. Clim. 33, 8339–8365. https://doi.org/10.1175/JCLI-D-19-0986.1.

Lombardo, F.T., Zickar, A.S., 2019. Characteristics of measured extreme thunderstorm near-surface wind gusts in the United States. J. Wind Eng. Ind. Aerod. 193, 103961 https://doi.org/10.1016/j.jweia.2019.103961.

Mandrekar, J.N., 2010. Receiver operating characteristic curve in diagnostic test assessment. J. Thorac. Oncol. 5 (9), 1315–1316. https://doi.org/10.1097/JTO.0b013e3181ec173d.

Market, P., Grempler, K., Sumrall, P., Henson, C., 2019. Analysis of severe elevated thunderstorms over frontal surfaces using DCIN and DCAPE. Atmosphere 10, 449. https://doi.org/10.3390/atmos10080449.

McCann, D.W., 1994. WINDEX—a new index for forecasting microburst potential. Weather Forecast. 9, 532–541. https://doi.org/10.1175/1520-0434(1994)009<0532:WNIFFM>2.0.CO;2.

McCarthy, J., Wilson, J.W., Fujita, T.T., 1982. The Joint airport weather studies project. Bull. Am. Meteorol. Soc. 63, 15–22. https://doi.org/10.1175/1520-0477(1982)063<0015:TJAWSP>2.0.CO;2.

McGovern, A., Lagerquist, R., Gagne, D.J., Jergensen, G.E., Elmore, K.L., Homeyer, C.R., Smith, T., 2019. Making the black box more transparent: understanding the physical implications of machine learning. Bull. Am. Meteorol. Soc. 100 (11), 2175–2199.

Miller, P.W., Mote, T.L., 2018. Characterizing severe weather potential in synoptically weakly forced thunderstorm environments. Nat. Hazards Earth Syst. Sci. 18, 1261–1277. https://doi.org/10.5194/nhess-18-1261-2018.

Miller, R.L., Ziegler, C.L., Biggerstaff, M.I., 2020. Seven-Doppler radar and in situ analysis of the 25–26 June 2015 Kansas MCS during PECAN. Mon. Weather Rev. 148, 211–240. https://doi.org/10.1175/MWR-D-19-0151.1.

NWS, 2021. National Weather Service Instruction 10-1605. Performance and Evaluation, NWSPD 10-16: Storm Data Preparation (Directive No. NWSI 10-1605). Department of Commerce, National Oceanic and Atmospheric Administration, National Weather Service, United States, Silver Spring, Maryland, United States. https://www.nws.noaa.gov/directives/sym/pd01016005curr.pdf.

Pacey, G.P., Schultz, D.M., Garcia-Carreras, L., 2021. Severe convective windstorms in Europe: climatology, preconvective environments, and convective mode. Weather Forecast. 36 (1), 237–252.

Pilguj, N., Taszarek, M., Allen, J.T., Hoogewind, K.A., 2022. Are Trends in Convective Parameters over the United States and Europe Consistent between Reanalyses and Observations? J. Clim. 35, 3605–3626. https://doi.org/10.1175/JCLI-D-21-0135.1.

Potvin, C.K., Broyles, C., Skinner, P.S., Brooks, H.E., Rasmussen, E., 2019. A Bayesian hierarchical modeling framework for correcting reporting bias in the U.S. tornado database. Weather Forecast. 34, 15–30. https://doi.org/10.1175/WAF-D-18-0137.1.

Púčik, T., Groenemeijer, P., Rýva, D., Kolář, M., 2015. Proximity soundings of severe and nonsevere thunderstorms in central Europe. Mon. Weather Rev. 143, 4805–4821. https://doi.org/10.1175/MWR-D-15-0104.1.

Richter, H., Peter, J., Collis, S., 2014. Analysis of a destructive wind storm on 16 November 2008 in Brisbane, Australia. Mon. Weather Rev. 142, 3038–3060. https://doi.org/10.1175/MWR-D-13-00405.1.

Romanic, D., Hangan, H., 2020. Experimental investigation of the interaction between near-surface atmospheric boundary layer winds and downburst outflows. J. Wind Eng. Ind. Aerod. 205, 104323 https://doi.org/10.1016/j.jweia.2020.104323.

Romanic, D., Hangan, H., Refan, M., Wu, C.-H., Michel, G., 2016. Oklahoma tornado risk and variability: a statistical model. Int. J. Disaster Risk Reduc. 16, 19–32. https://doi.org/10.1016/j.ijdrr.2016.01.011.

Romanic, D., Hangan, H., Chowdhury, J., Chowdhury, J., Hangan, H., 2020. Investigation of the transient nature of thunderstorm winds from Europe, the United States, and Australia using a new method for detection of changepoints in wind speed records. Mon. Weather Rev. 148, 3747–3771. https://doi.org/10.1175/MWR-D-19-0312.1.

Saha, S., Coauthors, 2014. The NCEP climate forecast system version 2. J. Clim. 27, 2185–2208. https://doi.org/10.1175/JCLI-D-12-00823.1.

Schaefer, J.T., Edwards, R., 1999. The SPC tornado/severe thunderstorm database. Preprints. In: 11th Conf. on Applied Climatology. Amer. Meteor. Soc., Dallas, TX, pp. 603–606.

Sherburn, K.D., Parker, M.D., King, J.R., Lackmann, G.M., 2016. Composite environments of severe and nonsevere high-shear, low-CAPE convective events. Weather Forecast. 31, 1899–1927. https://doi.org/10.1175/WAF-D-16-0086.1.

Smith, B.T., Thompson, R.L., Grams, J.S., Broyles, C., Brooks, H.E., 2012. Convective modes for significant severe thunderstorms in the contiguous United States. Part I: storm classification and climatology. Weather Forecast. 27, 1114–1135. https://doi.org/10.1175/WAF-D-11-00115.1.

Smith, B.T., Castellanos, T.E., Winters, A.C., Mead, C.M., Dean, A.R., Thompson, R.L., 2013. Measured severe convective wind climatology and associated convective modes of thunderstorms in the contiguous United States, 2003–09. Weather Forecast. 28, 229–236. https://doi.org/10.1175/WAF-D-12-00096.1.

Taszarek, M., Allen, J.T., Groenemeijer, P., Edwards, R., Brooks, H.E., Chmielewski, V., Enno, S.-E., 2020a. Severe convective storms across Europe and the United States. Part 1: climatology of lightning, large hail, severe wind and tornadoes. J. Clim. 1–47. https://doi.org/10.1175/JCLI-D-20-0345.1.

Taszarek, M., Allen, J.T., Groenemeijer, P., Edwards, R., Brooks, H.E., Chmielewski, V., Enno, S.-E., Púčik, T., Hoogewind, K.A., Brooks, H.E., 2020b. Severe convective storms across europe and the United States. Part 2: ERA5 environments associated with lightning, large hail, severe wind and tornadoes. J. Clim. 1–53 https://doi.org/10.1175/JCLI-D-20-0346.1.

Taszarek, M., Allen, J.T., Groenemeijer, P., Edwards, R., Brooks, H.E., Chmielewski, V., Enno, S.-E., Pilguj, N., Allen, J.T., Gensini, V., Brooks, H.E., Szuster, P., 2021. Comparison of convective parameters derived from ERA5 and MERRA-2 with rawinsonde data over Europe and North America. J. Clim. 34 (8), 3211–3237. https://doi.org/10.1175/JCLI-D-20-0484.1.

Tippett, M.K., Sobel, A.H., Camargo, S.J., Allen, J.T., 2014. An empirical relation between U.S. tornado activity and monthly environmental parameters. J. Clim. 27, 2983–2999. https://doi.org/10.1175/JCLI-D-13-00345.1.

Trapp, R.J., Wheatley, D.M., Atkins, N.T., Przybylinski, R.W., Wolf, R., 2006. Buyer beware: some words of caution on the use of severe wind reports in postevent assessment and research. Weather Forecast. 21, 408–415. https://doi.org/10.1175/WAF925.1.

Wakimoto, R.M., 1985. Forecasting dry microburst activity over the High Plains. Mon. Weather Rev. 113, 1131–1143. https://doi.org/10.1175/1520-0493(1985)113<1131:FDMAOT>2.0.CO;2.

Wilson, J.W., Roberts, R.D., Kessinger, C., McCarthy, J., 1984. Microburst wind structure and evaluation of Doppler radar for airport wind shear detection. J. Clim. Appl. Meteorol. 23, 898–915. https://doi.org/10.1175/1520-0450(1984)023<0898:MWSAEO>2.0.CO;2.

Wolfson, M.M., DiStefano, J.T., Forman, B.E., 1987. The FLOWS (FAA-Lincoln Laboratory Operational Weather Studies) Automatic Weather Station Network in Operation. Lincoln Laboratory, Massachusetts Institute of Technology. https://archive.ll.mit.edu/mission/aviation/publications/publication-files/atc-reports/Wolfson_1987_ATC-134_WW-15318.pdf.

Wolfson, M.M., Delanoy, R.L., Forman, B.E., Hallowell, R.G., Pawlak, M.L., Smith, P.D., 1995. Automated microburst wind-shear prediction. Linc. Lab. J. 7, 399–426.